

concurrent with the inversion at nitrogen. The barrier to inversion at the RHF level is 21.6 kJ mol<sup>-1</sup>, after inclusion of the zero-point vibrational energy correction. Introduction of the MP3 correlation correction raises the value to 27.1 kJ mol<sup>-1</sup>.

The instantaneous displacement vectors for the reaction coordinate at the transition structure describe motion with frequency 617.2i cm<sup>-1</sup> and are shown in Figure 4. As in the case of ammonia and aziridine, the deformation at the transition structure corresponds almost entirely to pyramidalization of the nitrogen atom. There are no significant components corresponding to puckering of the ring, rocking of the  $\alpha$ - or  $\beta$ -CH<sub>2</sub> groups, or twisting of the  $\alpha$ -CH<sub>2</sub> groups. These latter motions are coupled in modes with real frequencies, one of which is very low, 202.7 cm<sup>-1</sup>. Most of the loss of ZPVE which leads to the low inversion barrier for azetidine arises from differences in the frequencies of the lowest three vibrational modes of the equilibrium structure and the transition structure, including the mode with imaginary frequency in the latter.

### Conclusions

The temperature-dependent <sup>1</sup>H NMR spectrum of azetidine has been measured and analyzed to yield an estimate for the nitrogen inversion barrier:  $\Delta G^\ddagger$  (154 K) = 30 kJ mol<sup>-1</sup>. Approximate values for the activation enthalpy,  $\Delta H^\ddagger = 21 \pm 4$  kJ mol<sup>-1</sup>, and entropy,  $\Delta S^\ddagger = -45 \pm 25$  J mol<sup>-1</sup> K<sup>-1</sup>, were also

estimated. The equilibrium geometry and the geometry of the transition structure of azetidine were determined by ab initio RHF molecular orbital theory (Figures 1 and 2). The contribution of electron correlation energy was estimated to third order in Moller–Plesset perturbation theory (MP3), and the barriers were corrected for zero-point vibrational energy differences. The values of the barrier thus derived (RHF + ZPVE 21.6 kJ mol<sup>-1</sup>; MP3 + ZPVE 27.1 kJ mol<sup>-1</sup>) confirm that the inversion barrier in azetidine is low as is typical of unhindered amines and not elevated by angular constraints imposed by the ring, as happens in aziridine.

Unlike ammonia and aziridine, the normal vibrational mode with the lowest frequency in azetidine (Figure 3) does not lead directly along the reaction coordinate but rather involves deformation of the ring skeleton. In the transition structure of each of the three compounds, however, the normal mode with the imaginary frequency (Figure 4) involves almost exclusively out-of-plane motion of the NH bond and is therefore aligned with the reaction coordinate at the top of the barrier.

**Acknowledgment.** The financial support of the Natural Sciences and Engineering Sciences Research Council and of Control Data Corporation is gratefully acknowledged. The allocation of generous amounts of time on the University of Calgary's CDC Cyber 205 has made this work possible. One of us (R.D.) thanks the Killam Foundation for a Graduate scholarship.

## Influence of Disc–Rod–Sphere Phase Transitions in Nematic Lyotropics on a Unimolecular Isomerization Reaction

V. Ramesh and M. M. Labes\*

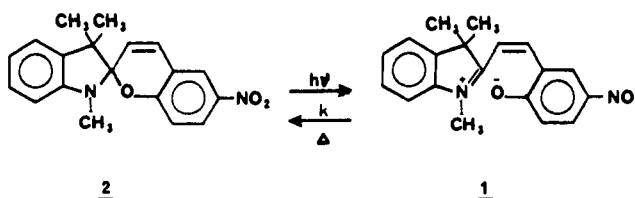
Contribution from the Department of Chemistry, Temple University, Philadelphia, Pennsylvania 19122. Received October 17, 1986

**Abstract:** The unimolecular isomerization of a photochromic merocyanine to an indolinospiropyran was performed in the nematic lyophases formed by potassium laurate (KL) or sodium decyl sulfate (SDS) with 1-decanol and water. In both systems there are discontinuities in reaction rates as a function of concentration or temperature which correspond to the phase transitions from disc- to rod- to sphere-like aggregates. Because of the change in molecular shape during the reaction, the order parameters of the reactant and products are quite different, and also reflect the differences between the rod- and disc-like phases in their ability to order the solute. The micropolarity and bulk viscosities of these phases are not very different, but microviscosity changes are the most likely explanation for the rate discontinuities at the phase transitions.

It has recently been established that bimolecular reactions conducted in nematic lyotropic liquid crystalline phases are profoundly influenced by the nature of the aggregate.<sup>1</sup> Such nematic lyotropic phases consist of either cylindrical (N<sub>C</sub>) or disk-like (N<sub>D</sub>) aggregates, and a phase transition can occur between them by changing either the temperature of the system or the concentration of one of the phase constituents.<sup>2</sup> The isotropic (I) phases of these same systems are thought to consist of conventional spherical micellar aggregates. Thus, in typical experiments disc–rod–sphere transitions can be examined with respect to their influence on kinetics and products of a variety of reactions.

Several factors can be involved in modulating the reactivity of a solute in these media; the local order, polarity, viscosity, as well as the sites of solubilization may change with aggregate size and shape. To simplify the problem, we undertook a study of a

Scheme I



unimolecular reaction—the isomerization of a photochromic merocyanine **1** to an indolinospiropyran **2** (Scheme I)—in two nematic lyophases. The first phase consists of potassium laurate (KL), 1-decanol, and water, whereas the second contains sodium decyl sulfate (SDS), 1-decanol, and water. The phase diagrams of these systems have been studied in detail,<sup>4,5</sup> and both have easily

(1) (a) Ramesh, V.; Labes, M. M. *J. Am. Chem. Soc.* **1986**, *108*, 4643. (b) Ramesh, V.; Labes, M. M. *Mol. Cryst. Liq. Cryst.*, in press. (2) Forrest, B. J.; Reeves, L. W. *Chem. Rev.* **1981**, *81*, 1 and references therein.

(3) Brown, G. H., Ed.; *Photochromism: Techniques of Chemistry*; Wiley-Interscience: New York, 1971; Vol. III. (4) Yu, L. J.; Saupe, A. *Phys. Rev. Lett.* **1980**, *45*, 1000.

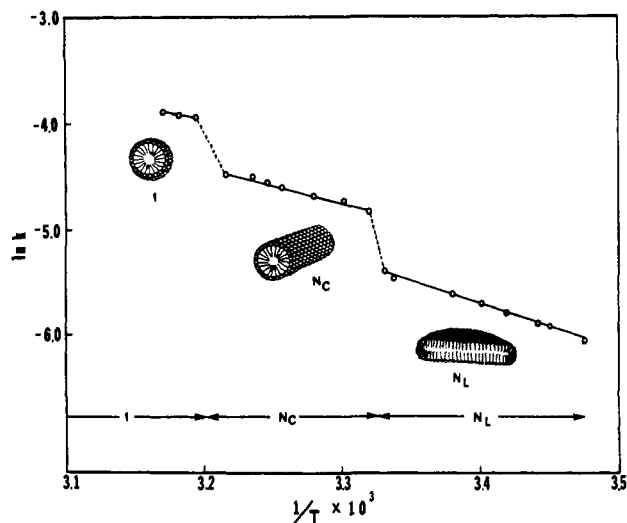


**Figure 1.** Arrhenius plot of the merocyanine to spiropyran isomerization in the  $N_L$ ,  $N_C$ , and I phases of KL/water/1-decanol (26.0/66.76/6.24 wt%).

accessible  $N_C$ ,  $N_L$ , and I phases at convenient temperatures and concentrations.

Not only were the rate constants ( $k$ ) of the isomerization measured, but we were also able to determine the "order parameter"  $S$  (the degree of orientational ordering with respect to the nematic lyophases) of both the reactant and product. In addition, to ascertain the micropolarity encountered by **1** in the  $N_L$ ,  $N_C$ , and I phases, we measured the absorption maxima for merocyanine in these phases and compared them with solvents of known polarity.

### Experimental Section

**Materials.** 1',3',3'-Trimethyl-6-nitrospiro[2*H*-benzopyran-2,2'-indoline] (**2**) was obtained from CTC Organics and recrystallized from absolute ethanol, mp 178–179 °C (lit.<sup>6</sup> 180 °C). SDS, obtained from Aldrich Chemical Co., was recrystallized two times from 95% ethanol/water and dried under vacuum. KL was synthesized and purified by literature methods.<sup>7</sup> Triply distilled water was used in the preparation of all samples.

**Kinetic Studies.** A  $7 \times 10^{-4}$  M solution of **2** in the liquid crystalline solvents (either SDS/1-decanol/water or KL/1-decanol/water) was prepared by stirring together for 12 h weighed amounts of **2** and the components forming the lyomesophases. The  $N_L$ - $N_C$  and  $N_C$ -I transitions were depressed by approximately 1 °C in these solutions. These phase transitions could easily be observed by examining the samples on a Nikon polarizing microscope on a Mettler FP-52 hot stage. The  $N_C$  phase shows a typical nematic schlieren texture, whereas  $N_L$  phases are best identified conoscopically because of their spontaneous homeotropic texture. A 0.5-g portion of solution was introduced into a 1-mm path length UV cuvette and thermostated for 10 min at the appropriate temperature in the range 15.5–40 °C. Each sample was irradiated for ca. 1 min using a 25-W spectroline low-pressure Hg vapor pencil lamp and a Corning CS 7-54 filter to photochemically generate **1** from **2**. A Perkin-Elmer 330 spectrophotometer interfaced with a Model 3600 data station was used to monitor the isomerization of **1** at 530 nm for KL samples and 522 nm for SDS samples. Isomerization rate constants ( $k$ ) were obtained from computer-generated correlations of  $\ln(OD_t - OD_\infty)$  with time, where  $OD_t$  and  $OD_\infty$  are the optical densities at any given time  $t$ , and at time  $t = 15$  h, respectively. At least three independent experiments were conducted at each temperature and the mean value for  $k$  was determined. Errors in the rate constants were  $\pm 4\%$ .

The order parameter,  $S$ , for **1** and **2** in KL and SDS lyomesophases were determined by polarized absorption spectroscopy.<sup>8</sup> The nematic phases ( $N_L$  and  $N_C$ ) were aligned by placing the samples in a 15-kG magnetic field overnight, so that the nematic director  $\bar{n}$  was coincident with the long axis of the spectroscopic cell, a conventional 1-mm UV cuvette. Absorbances parallel and perpendicular to  $\bar{n}$  were determined

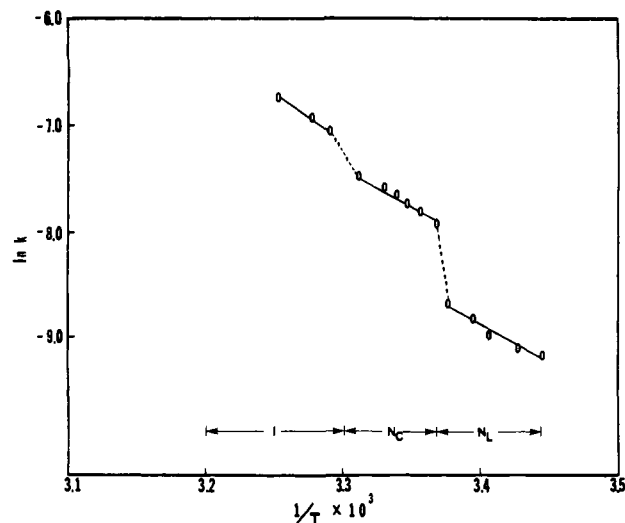


**Figure 2.** Arrhenius plot of the merocyanine to spiropyran isomerization in the  $N_L$ ,  $N_C$ , and I phases of SDS/water/1-decanol (35/58/7 wt%).

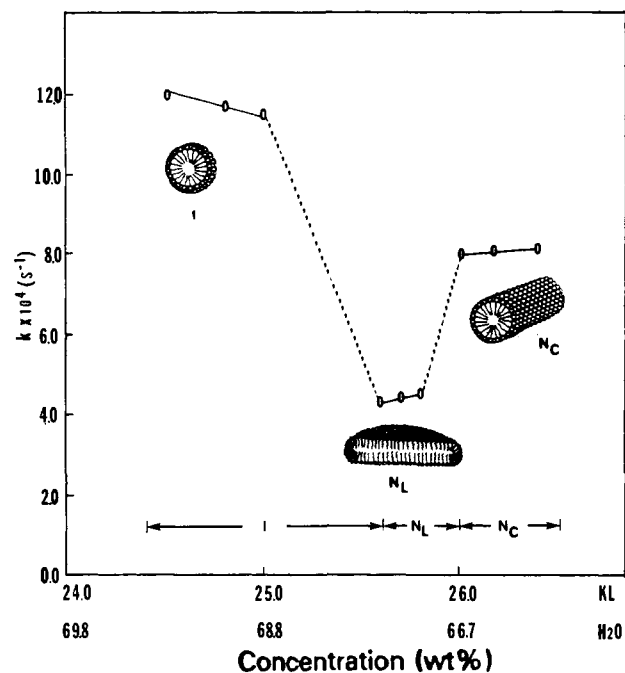


**Figure 3.** Isomerization rate constants  $k$  ( $s^{-1}$ ) as a function of KL/water concentration at 28 °C, and at constant 1-decanol concentration (6.24 wt%).

using a Perkin-Elmer 330 spectrometer interfaced with a Model 3600 data station and fitted with Glan-Foucault polarizers.

### Results and Discussion

The thermal isomerization of merocyanine **1** to spiropyran **2** in  $N_L$ ,  $N_C$ , and I phases of KL and SDS exhibited simple first-order kinetics. Computer-generated correlations of  $\ln(OD_t - OD_\infty)$  vs. time were linear over at least two half-lives with correlation coefficients  $r > 0.99$ . It is noteworthy that the kinetics of isomerization of **1**  $\rightarrow$  **2** in lyomesophases of KL and SDS are analogous to those in polar solvents like ethanol<sup>9</sup> and are in contrast to those in solid matrices (e.g., poly(alkyl methacrylate) films<sup>10</sup>) where complex first-order kinetics were observed.

Plots of isomerization rate constants  $k$  as a function of temperature (Arrhenius plots) and as a function of concentration for the KL and SDS lyomesophases are depicted in Figure 1–4. The experimental values for the phase-transition temperatures de-

(5) Yu, L. J.; Saupe, A. *J. Am. Chem. Soc.* **1980**, *102*, 4879.

(6) Hinnen, A.; Audic, C.; Gautron, R. *Bull. Soc. Chim. Fr.* **1968**, 2066.

(7) Saupe, A.; Boonbrahm, P.; Yu, L. J. *J. Chim. Phys.* **1983**, *80*, 7.

(8) (a) Kuzma, M.; Skarda, V.; Labes, M. M. *J. Chem. Phys.* **1984**, *81*, 2925. (b) Skarda, V.; Labes, M. M. *Mol. Cryst. Liq. Cryst.* **1985**, *126*, 187.

(9) Berman, E.; Fox, R. E.; Thomson, F. D. *J. Am. Chem. Soc.* **1959**, *81*, 5605.

(10) Gardlund, Z. G.; Laverty, J. J. *Polym. Lett.* **1969**, *7*, 719.

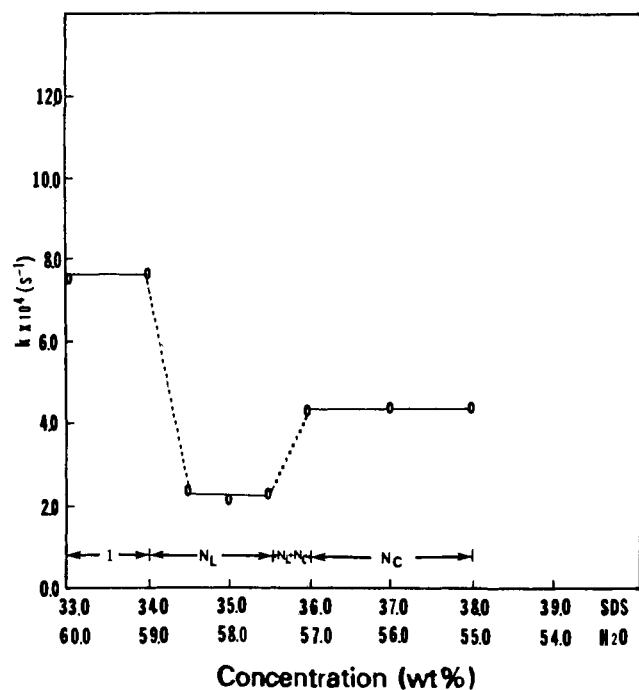


**Figure 4.** Isomerization rate constants  $k$  ( $s^{-1}$ ) as a function of SDS/water concentration at 20 °C, and at constant 1-decanol concentration (7 wt%).

terminated optically are indicated on each plot. The most striking observation is that in both systems there are marked discontinuities in reaction rates as a function of concentration or temperature which correspond to the phase transitions from disc- to rod- to sphere-like aggregates. Of particular significance is the retardation in isomerization rate by the  $N_L$  phase. While the rate of isomerization is affected by the nature of the surfactant aggregate, no significant changes in activation energy through the phase transitions are observed. For example,  $E_{act}$  is  $\sim 8.5$  kcal mol $^{-1}$  in KL and  $\sim 13.3$  kcal mol $^{-1}$  in SDS regardless of whether the phase is  $N_L$ ,  $N_C$ , or I.<sup>11</sup>

At least three factors can influence the reactivity of **1** toward ring closure: polarity, viscosity, and local order of the aggregate where molecules of **1** are solubilized. Solvent polarity is extremely important in determining the rates and mechanism of **1**  $\rightarrow$  **2** isomerization.<sup>3,12</sup> Polar solvents stabilize the zwitterionic merocyanines and retard ring closure. In order to ascertain whether micropolarity differences between the bilayer ( $N_L$ ), cylindrical ( $N_C$ ), and spherical (I) surfactant aggregates are responsible for the observed rate changes, the micropolarity encountered by **1** in these aggregates was determined.

The absorption maximum of **1** corresponds to transition from a predominantly dipolar ground state to an excited state of considerably reduced polarity.<sup>13</sup> As the polarity of the solvent increases, the dipolar ground state is more stabilized than the excited state, and consequently the intense, well-resolved long wavelength absorption band of **1** moves to higher energy with increasing solvent polarity. The sensitivity of  $\lambda_{max}$  of **1** to changes in solvent polarity was used to determine the micropolarity of the  $N_L$ ,  $N_C$ , and I phases.<sup>14,15</sup>

Since **1** is almost insoluble in water and dilute surfactant solutions but soluble in lyomesophases, it is ideally suited to probe the lyomesophase micropolarity, since problems associated with the distribution of the probe between the aqueous and the micellar phase do not arise. The  $\lambda_{max}$  and corresponding transition energy ( $E_{sp}$ ) of **1** in a variety of solvents and in the  $N_L$ ,  $N_C$ , and I phases

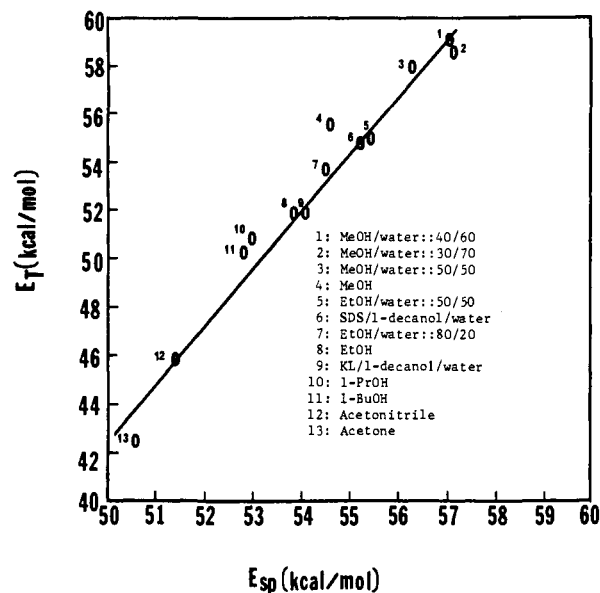


**Figure 5.** Plot of  $E_T$  vs.  $E_{sp}$  for merocyanine absorption in various organic solvents and in lyomesophases.

**Table I.** Order Parameters  $S$  and  $\lambda_{max}$  for Merocyanine **1** and Spiropyran **2** in the  $N_L$  and  $N_C$  Phases<sup>a</sup> for KL and SDS Lyomesophases

compound	lyomesophase	$N_L$		$N_C$	
		$\lambda_{max}$ , nm	$S$	$\lambda_{max}$ , nm	$S$
merocyanine <b>1</b>	KL/1-dec/H <sub>2</sub> O	530	-0.053	530	-0.099
	SDS/1-dec/H <sub>2</sub> O	522	-0.046	522	-0.099
spiropyran <b>2</b>	KL/1-dec/H <sub>2</sub> O	354	-0.002	354	-0.003
		244		244	
	SDS/1-dec/H <sub>2</sub> O	354	-0.002	354	-0.003
		244		244	

<sup>a</sup>  $\lambda_{max}$  values for **1** in the isotropic micellar phase (I) of KL and SDS are 530 and 522 nm, respectively.

of KL and SDS were determined. A plot of  $E_{sp}$  against the well-established standard polarity parameter,<sup>16</sup>  $E_T$ , is shown in Figure 5. A good correlation between  $E_{sp}$  and  $E_T$  was obtained substantiating the validity of **1** as a polarity probe.<sup>14,15</sup>  $\lambda_{max}$  values for the  $N_L$ ,  $N_C$ , and I phases of KL and SDS are shown in Table I. Since  $\lambda_{max}$  does not shift through the phase transitions, the micropolarity experienced by **1** in the bilayer, cylindrical, and spherical aggregates appears to be identical. Therefore, it is reasonable to conclude that micropolarity differences are not involved in the reactivity modulation of **1** with change in the nature of surfactant aggregate.

The degree of orientational ordering of a solute with respect to a liquid crystalline solvent is evaluated in terms of an order parameter  $S$ .<sup>17-19</sup> When an anisotropic optical property such as absorbance is measured, the order parameter is given by

$$S = (A_{\parallel} - A_{\perp}) / A_{\parallel} + 2A_{\perp}$$

Here we define  $A_{\parallel}$  and  $A_{\perp}$  as the absorbance parallel and perpendicular to the optic axis or nematic director.

Order parameter values, determined by polarized absorption spectroscopy for both **1** and **2** in the  $N_L$  and  $N_C$  phases of SDS and KL are shown in Table I. Low  $S$  values for **2** and high  $S$  values for **1** are an indication that the degree of orientational ordering for the globular spiropyran molecules is low, while that

(11) Enthalpy and entropy values can also be calculated but, because of the small accessible temperature range, are inherently inaccurate.

(12) Flannery, J. B., Jr. *J. Am. Chem. Soc.* **1968**, *90*, 5660.

(13) Kosower, E. M. *J. Am. Chem. Soc.* **1958**, *80*, 3253.

(14) Zachariasse, K. A.; Phuc, N. V.; Kozankiewicz, B. *J. Phys. Chem.* **1981**, *85*, 2676.

(15) deMayo, P.; Amiri, A. S.; Wong, S. K. *Can. J. Chem.* **1984**, *62*, 1001.

(16) Reichardt, C. *Angew. Chem., Int. Ed. Engl.* **1965**, *4*, 29

(17) Neff, V. D.; Gulrich, L. W.; Brown, G. H. In *Liquid Crystals*; Brown, G. H., Dienes, G. J., Labes, M. M., Eds.; Gordon and Breach: New York, 1966; p 21.

(18) Neff, V. D. In *Liquid Crystals and Plastic Crystals*; Gray, G. W., Winsor, P. A., Eds.; Ellis Horwood: Chichester, U. K., 1974; pp 2, 231.

(19) Maier, W.; Englert, G. *Z. Elektrochem.* **1960**, *64*, 689.

for the rod-shaped merocyanine molecules is much higher. Further, the large change in  $S$ , in going from **1** to **2**, is indicative of the significant molecular motion required during the reaction. Therefore, the constraints offered by the local order encountered by **1** in the aggregate cannot be ignored. Since rates of  $\mathbf{1} \rightarrow \mathbf{2}$  isomerization are lowest in the  $N_L$  phase, it is obvious that the bilayer nature of the disc-like aggregate offers the most constraint to ring closure. This could most probably arise because of the rod-like merocyanine molecules being effectively "incorporated" within the bilayer matrix preventing facile ring closure. In fact, a similar explanation has been advanced to explain the retardation of isomerization rates of **1** in the smectic B phase of *n*-butyl stearate.<sup>20</sup>

The kinetics of merocyanine to spiropyran isomerization have been studied in three polybutadiene oligomers<sup>20</sup> and in a variety of polymeric media.<sup>21-23</sup> Although no clear-cut dependence of isomerization rates on viscosity has been established, it appears that isomerization rates are not significantly altered by the bulk viscosity of the solvent. However, the internal or microviscosity arising from restricted segmental motions of the hydrocarbon chains in the vicinity of merocyanine molecules does appear to play a significant role in determining the rates and mechanism of the isomerization.<sup>20-23</sup> The bulk viscosities for KL and SDS lyomesophases have been determined.<sup>24,25</sup> No significant changes

in viscosity at the  $N_L \rightarrow N_C$  transitions are observed, but viscosity decreases drastically at the  $N_C \rightarrow I$  transitions.

Lower bulk viscosity in the isotropic micellar phase (I) could enhance freedom for molecular motion in **1** and consequently isomerization rates are expected to be and are higher in the I phase as compared to  $N_L$  or  $N_C$  phases. The microviscosities of the bilayer and cylindrical aggregates are not known. Depending upon the site where **1** is solubilized in the disc-like and cylindrical aggregates, the microviscosity encountered by **1** could be quite different, and this could contribute significantly to the reactivity of **1**.

### Conclusions

The rates of the unimolecular rearrangement of a merocyanine to a spiropyran in nematic lyophases are dependent on the nature of the surfactant aggregate. The lowest rates are encountered in the disc-like  $N_L$  phase. Since the wavelength of absorption maximum for the merocyanine does not change through the phase transitions, the polarity of  $N_C$ ,  $N_L$ , and I phases appear to be identical. There is a large change in the order parameters of reactant and product indicative of the significant molecular motion required during the reaction. Although the bulk viscosities of  $N_L$  and  $N_C$  phases are not very different, microviscosities are probably quite different. This difference coupled with the changes in local order encountered by **1** are the most likely explanations for the rate changes at the phase transitions.

**Acknowledgment.** This work was supported by the U.S. Army Research Office, under Contract No. DAAG29-84-K-0036.

- (20) Otruba, J. P., III; Weiss, R. G. *Mol. Cryst. Liq. Cryst.* **1982**, *80*, 165.  
 (21) Gardlund, Z. G. *Polym. Lett.* **1968**, *6*, 57.  
 (22) Vandeweyer, P. H.; Smetz, G. J. *Polym. Sci., Part A-1.* **1970**, *8*, 2361.  
 (23) Kryszewski, M.; Lapienis, D.; Nadolski, B. *J. Polym. Sci., Polym. Chem. Ed.* **1973**, *11*, 2423 and references therein.  
 (24) Roy, M.; McClymer, J. P.; Keyes, P. H. *Mol. Cryst. Liq. Cryst. Lett.* **1985**, *1*, 25.

- (25) Hui, Y. W.; Labes, M. M., (unpublished results).

## Reaction Path Analysis of Hydrogen Abstraction by the Formaldehyde Triplet State<sup>1</sup>

Daniel Severance, Bipin Pandey, and Harry Morrison\*

Contribution from the Department of Chemistry, Purdue University, West Lafayette, Indiana 47907. Received January 2, 1987

**Abstract:** The fully optimized transition state for hydrogen abstraction from methane by the formaldehyde excited triplet state has been determined by using ab initio theory and UHF/3-21G calculations. The most noteworthy feature of the transition state is that the methane hydrogen approaches the oxygen at an angle of 108.9° rather than at the 90° normally assumed for this reaction. Steric factors are suggested as the most likely source of this observation.

### I. Introduction

Theoretical analysis of the preferred trajectory for attack on a carbonyl group by nucleophiles has become a powerful tool for understanding a wide array of ketone and aldehyde ground-state chemistry.<sup>2</sup> By comparison, relatively little computational effort has been devoted to defining the preferred mode of approach of reactants toward the carbonyl excited-state. For example, theoretical discussions have generally assumed that  $\theta$  (Figure 1) for the prototypical hydrogen abstraction reaction by a formaldehyde  $^3n-\pi^*$  state is 90°<sup>3</sup> (as would be expected for the initial approach

of a hydrogen donor to the nonbonding p-orbital of the sp hybridized oxygen<sup>4,5</sup>). There is a corresponding paucity of excited-state experimental data vis-a-vis the  $\rho$ ,  $\theta$ , and  $\phi$  parameters of Figure 1. What is available is derived from intramolecular chemistry and limited by the constraints thus imposed.<sup>6</sup> We have therefore undertaken a theoretical study of hydrogen abstraction by the formaldehyde triplet state in order to define the preferred transition state for approach by methane. This is the first treatment of this reaction which involves full optimization to give the saddle point geometry.

- (1) Organic Photochemistry. 71. Part 70: Morrison, H.; De Cardenas, L. *J. Org. Chem.*, in the press.  
 (2) Liotta, C. L.; Burgess, E. M.; Eberhardt, W. H. *J. Am. Chem. Soc.* **1984**, *106*, 4849-4852 and references therein.  
 (3) (a) Bigot, B. *Isr. J. Chem.* **1983**, *23*, 116-123 and reference therein  
 (b) Chandra, A. K. *J. Photochem.* **1979**, *11*, 347-360.

- (4) Jorgensen, W.; Salem L. *The Organic Chemist's Book of Orbitals*; Academic Press: New York, 1973, p 84.  
 (5) Zimmerman, H. E. *Acc. Chem. Res.* **1982**, *10*, 312.  
 (6) Examples include (a) Lewis, F. D.; Johnson, R. W.; Ruden, R. A. *J. Am. Chem. Soc.* **1972**, *94*, 4292-4297. (b) Scheffer, J. R.; Trotter, J.; Nalamasu, O.; Evans, S. V.; Ariel, S. *Mol. Cryst. Liq. Cryst.* **1986**, *134*, 169-196.